© 2014. Published by The Company of Biologists Ltd | Development (2014) 141, 4513-4525 doi:10.1242/dev.109124

RESEARCH ARTICLE

The lipoprotein receptor LRP1 modulates sphingosine-1-phosphate signaling and is essential for vascular development

Chikako Nakajima[1,2,3,4,*], Philipp Haffner[2,*], Sebastian M. Goerke[2,5,*], Kai Zurhove[1,2], Giselind Adelmann[6], Michael Frotscher[7], Joachim Herz[2,8], Hans H. Bock[1,2,4] and Petra May[1,2,4,‡]

ABSTRACT

Low density lipoprotein receptor-related protein 1 (LRP1) is indispensable for embryonic development. Comparing different genetically engineered mouse models, we found that expression of *Lrp1* is essential in the embryo proper. Loss of LRP1 leads to lethal vascular defects with lack of proper investment with mural cells of both large and small vessels. We further demonstrate that LRP1 modulates Gi-dependent sphingosine-1-phosphate (S1P) signaling and integrates S1P and PDGF-BB signaling pathways, which are both crucial for mural cell recruitment, via its intracellular domain. Loss of LRP1 leads to a lack of S1P-dependent inhibition of RAC1 and loss of constraint of PDGF-BB-induced cell migration. Our studies thus identify LRP1 as a novel player in angiogenesis and in the recruitment and maintenance of mural cells. Moreover, they reveal an unexpected link between lipoprotein receptor and sphingolipid signaling that, in addition to angiogenesis during embryonic development, is of potential importance for other targets of these pathways, such as tumor angiogenesis and inflammatory processes.

KEY WORDS: Lipoprotein receptor, Sphingolipid, Angiogenesis

INTRODUCTION

During vertebrate embryonic development the formation of blood vessels by vasculogenesis and angiogenesis leads to the establishment of blood circulation (Adams and Alitalo, 2007). For the circulation to be adequately maintained throughout development and in postnatal life, blood vessels need to mature, i.e. they need to be invested with mural cells for support and stability (Gaengel et al., 2009). This involves the differentiation of pericytes and vascular smooth muscle cells, collectively called mural cells, from mesenchymal precursors, their recruitment to developing blood vessels, and their adequate proliferation. Some crucial mechanisms that regulate this complex process have been identified: PDGF-BB secreted by endothelial cells and acting via PDGF receptor-β (PDGFRβ) on mural cells plays an essential role in recruiting pericytes/vascular smooth muscle cells and maintaining vascular stability (Hellstrom et al., 1999; Bjarnegard et al., 2004). A related function, which is likely to involve modulation of the PDGF-BB–PDGFRβ signaling axis, is carried out by sphingosine-1-phosphate (S1P) and the components of its signaling network (Liu et al., 2000; Hobson et al., 2001; Mizugishi et al., 2005). Of the five S1P receptors, $S1P_1$ (also known as EDG1 or S1PR1) seems to play the predominant role during vascular development. It is highly expressed on endothelial cells and to a lesser extent also on vascular smooth muscle cells, on which $S1P_2$ (EDG5 or S1PR2) is more prominent (Allende and Proia, 2002; Kluk and Hla, 2002; Ryu et al., 2002).

The transmembrane receptor LRP1 is a member of the low density lipoprotein (LDL) receptor family of lipoprotein receptors. It is expressed ubiquitously in the adult and has dual functions in endocytosis and signal transduction (May et al., 2005; Lillis et al., 2008). Examination of mice lacking LRP1 in smooth muscle cells, including differentiated vascular smooth muscle cells, revealed that the receptor is essential for the integrity of the vascular wall. On the one hand, it confers protection from cholesterol-induced atherosclerosis independently of systemic cholesterol levels (Boucher et al., 2003). On the other hand, it controls PDGF-BB and TGFβ signaling in vascular smooth muscle cells and thus prevents their overproliferation and disruption of their normal layering (Boucher et al., 2007). Its role during vascular development is less clear owing to the early embryonic lethality of conventionally genetically engineered *Lrp1*-deficient mice (Herz et al., 1992). Although the initial hypothesis that $Lrp1^{-/-}$ embryos die before implantation into the uterus was amended to embryonic lethality during early to mid-gestation (Herz et al., 1993), its actual function during embryonic development is yet to be elucidated. Also, it is unclear whether LRP1 exerts its essential functions in the embryo proper or whether its main role is in the supporting extraembryonic tissues, where it could serve in cargo transport across the placenta owing to its ability to endocytose extracellular ligands.

Here, we examined mice that lack *Lrp1* either completely or in the embryo proper only. We show that *Lrp1* has an essential role in the embryo proper and that *Lrp1* expression in the supporting tissues is insufficient to rescue embryonic development. Morphological and immunohistochemical analyses of $Lrp1^{-/-}$ embryos reveal an essential role of LRP1 in blood vessel maturation, as proper investment with mural cells does not occur in these animals. The vascular defects result in widespread hemorrhage and subsequent circulatory failure and ultimately in the death of the embryos at ~E13.5. *In vitro* examination of mesenchymal cell migration and signal transduction in both fibroblasts and endothelial cells reveals a regulatory role of LRP1

[1]Department of Medicine II, University Hospital and University of Freiburg, 79106 Freiburg, Germany. [2]Centre for Neurosciences, University Hospital and University of Freiburg, 79104 Freiburg, Germany. [3]Institute of Physiological Chemistry and Focus Program Translational Neuroscience (Adult Neurogenesis and Cellular Reprogramming), University Medical Center, Johannes Gutenberg University Mainz, 55128 Mainz, Germany. [4]Department of Gastroenterology, Hepatology and Infectiology, University Hospital of Düsseldorf, 40225 Düsseldorf, Germany. [5]Department of Plastic and Hand Surgery, University Hospital and University of Freiburg, 79106 Freiburg, Germany. [6]Institute of Anatomy and Cell Biology, University Hospital and University of Freiburg, 79104 Freiburg, Germany. [7]Institute for Structural Neurobiology, Center for Molecular Neurobiology Hamburg, University Medical Center Hamburg-Eppendorf, 20251 Hamburg, Germany. [8]Department for Molecular Genetics, University of Texas Southwestern Medical Center at Dallas, Dallas, TX 75390, USA.
*These authors contributed equally to this work

[‡]Author for correspondence (petra.may@med.uni-duesseldorf.de)

Received 17 February 2014; Accepted 4 September 2014

Development (2014) 141, 4513-4525 doi:10.1242/dev.109124

in Gi-dependent S1P signaling and in the crosstalk of the S1P and PDGF-BB pathways, which requires the LRP1 intracellular domain and seems to underlie the vascular developmental defect observed in *Lrp1*$^{-/-}$ animals.

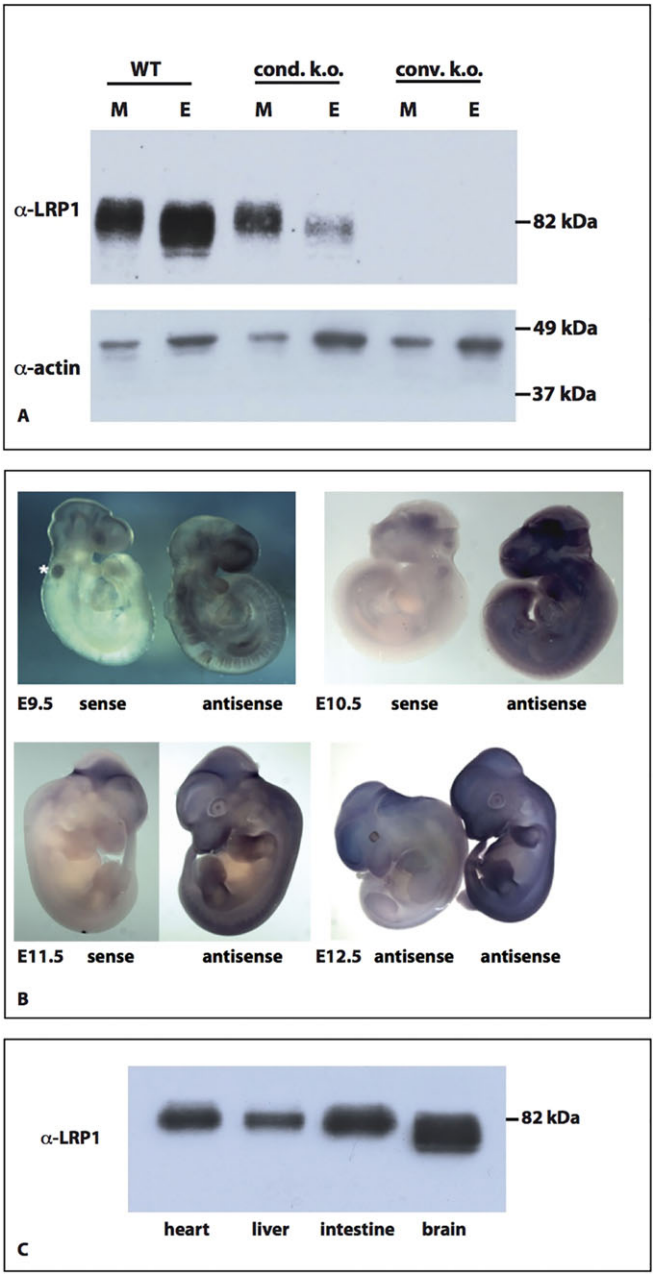

Fig. 1. LRP1 expression in the experimental mouse lines. (A) Lysates of *Lrp1*-containing (WT: LRP1$^{lox/lox}$), conditionally *Lrp1*-deficient (cond. k.o.: MeoxCre-LRP1$^{rec/lox}$) and conventionally *Lrp1*-deficient (conv. k.o.: LRP$^{rec/rec}$) embryos (E) and membranes (M) were prepared. 40 µg protein was separated by SDS-PAGE and analyzed by western blotting and staining with an LRP1 antibody. Staining with an actin antibody served as loading control. (B) Embryos of different ages were prepared from time-mated pregnant mice and examined by whole-mount *in situ* hybridization with an *Lrp1* antisense probe. The corresponding sense probe or examination of *Lrp1*$^{-/-}$ embryos served as controls. Wild-type embryos were examined at E9.5, E10.5 and E11.5 (sense probe left, antisense right). E12.5 *Lrp1*$^{-/-}$ (left) and wild-type (right) embryos examined with antisense probe. (C) Various organs were prepared from E12.5 wild-type embryos. Organ lysates were analyzed by SDS-PAGE, western blotting and staining with LRP1 antibody.

RESULTS

LRP1 plays an essential role during development of the embryo proper

In order to clarify the role of LRP1 during embryonic development, we crossed mice with floxed *Lrp1* alleles to knock-in mice that express Cre recombinase under the control of the *Meox2* promoter. The *Meox2* promoter is activated in the epiblast (Tallquist and Soriano, 2000) and thus leads to Cre expression and subsequent recombination of floxed alleles in all tissues of the embryo proper, whereas the extraembryonic tissues are spared.

Comparison of conditionally *Lrp1*-deficient MeoxCre-LRP1$^{rec/lox}$ embryos with embryos with completely recombined *Lrp1* alleles (LRP1$^{rec/rec}$) confirmed a lack of LRP1 protein in extraembryonic membranes and the embryo proper of LRP1$^{rec/rec}$ offspring. By contrast, in MeoxCre-LRP1$^{rec/lox}$ LRP1 is preserved in the extraembryonic tissues but is almost completely absent from the embryo proper (Fig. 1A). Neither genotype was found in newborn offspring from suitable matings and genotyping of timed embryos revealed that LRP1$^{rec/rec}$ embryos die after E11.5 with no living LRP1$^{rec/rec}$ conceptus left after E13.5 (Table 1). MeoxCre-LRP1$^{rec/lox}$ embryos show a similar decline that begins after E12.5, with complete loss by E14.5.

These findings indicate that preservation of LRP1 in the extraembryonic tissues cannot rescue *Lrp1*$^{-/-}$ embryos from their lethal developmental defects and point to an essential developmental role for LRP1 in the embryo proper.

LRP1 is expressed ubiquitously during embryonic development

E9.5-12.5 wild-type embryos were examined by whole-mount *in situ* hybridization with an antisense probe specific for the *Lrp1* mRNA. Comparison of these embryos with *Lrp1*$^{-/-}$ controls and wild-type controls stained with a sense probe revealed ubiquitous expression of *Lrp1* mRNA during all stages examined (Fig. 1B). Western blotting confirmed LRP1 expression in the developing brain as well as in heart, liver and intestine (Fig. 1C). Interestingly, the LRP1 protein already exhibited the organ-dependent variation in apparent size that is observed in adult animals and occurs due to differential glycosylation (May et al., 2003).

Severe vascular defects underlie the embryonic lethality of *Lrp1* deficiency

Macroscopic morphological analysis of *Lrp1*-deficient LRP1$^{rec/rec}$ embryos revealed extensive hemorrhage (Fig. 2A-C). Bleeding

Table 1. Survival of conditionally and completely *Lrp1*-deficient embryos

	E11.5	E12.5	E13.5	E14.5
Conventional k.o.				
k.o. expected (%)	25	25	25	
k.o. observed (%)	23	27	22	
k.o. alive (%)	23	19	0	
Number of animals	48	198	36	
Conditional k.o.				
k.o. expected (%)		25	25	25
k.o. observed (%)		20	35	24
k.o. alive (%)		20	10	0
Number of animals		35	51	38

Embryos of time-mated mice were assessed for viability and genotyped at the time points indicated. Matings were: MeoxCre-LRP1$^{wt/rec}$×LRP1$^{lox/lox}$ for conditionally *Lrp1*-deficient embryos and LRP1$^{lox/rec}$×LRP1$^{lox/rec}$ for completely *Lrp1*-deficient embryos. The total number of embryos examined is given for each day.
k.o., knockout.

Development (2014) 141, 4513-4525 doi:10.1242/dev.109124

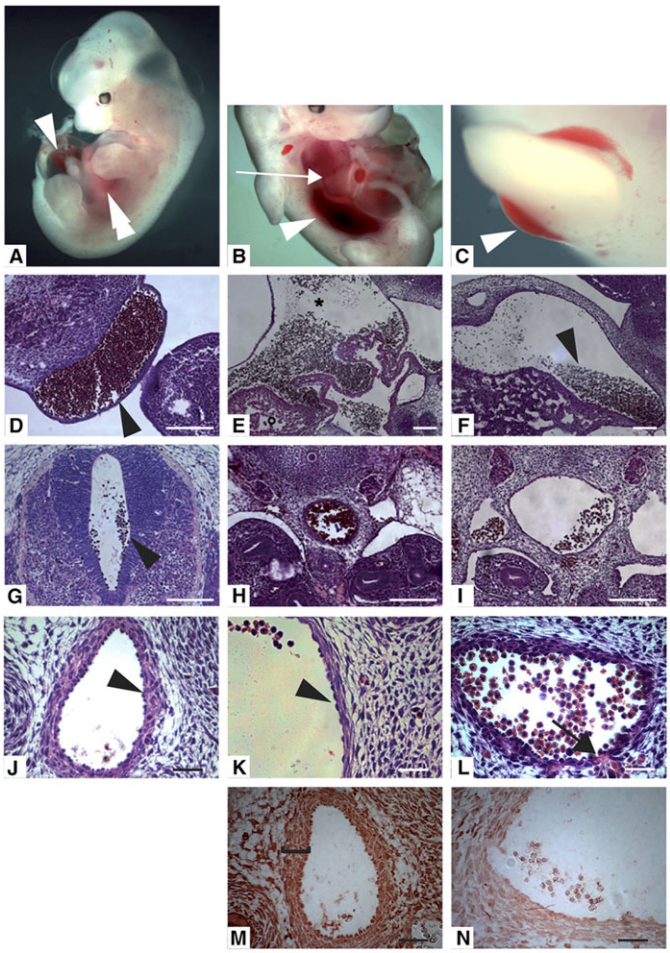

Fig. 2. Widespread hemorrhage due to vascular anomalies in *Lrp1*-deficient mice. (A-C) E12.5 *Lrp1*-deficient embryo showing: (A) bleeding into the umbilical cord (arrowhead), into the pericardium, and into the subcutaneous tissue (double arrowhead); (B) extensive hemorrhage in the pleural (arrow) and abdominal cavities (arrowhead); (C) subcutaneous hemorrhage along an extremity (arrowhead). (D-F) HE-stained paraffin section of E12.5 *Lrp1*-deficient embryo showing: (D) bullous subcutaneous hemorrhage (arrowhead); (E) hematopericardium (asterisk) (circle marks ventricle); (F) hematoperitoneum (arrowhead). In the lower left corner the liver is visible. (G-N) Paraffin-embedded E12.5 tissues were sectioned coronally and stained with HE (G-L) or analyzed by immunohistochemistry (M,N). (G) *Lrp1*-deficient embryo showing blood in the neural canal (arrowhead). (H) Wild-type embryo with the aorta at the center. (I) $Lrp1^{-/-}$ embryo with the aorta at the center. (J) Wild-type embryo showing the aorta (arrowhead). (K) $Lrp1^{-/-}$ embryo showing the dilated aorta (arrowhead). (L) $Lrp1^{-/-}$ embryo showing the aorta; the arrow points to a discontinuity in the endothelium and blood cells in the surrounding tissue. (M) Wild-type and (N) $Lrp1^{-/-}$ embryos were analyzed by immunohistochemistry with an anti-desmin antibody. Bound antibody was visualized with a chromogenic substrate for horseradish peroxidase via the avidin/extravidin system. Bracket indicates the smooth muscle cell layers of the aortal wall. Scale bars: 100 µm in A-I; 20 µm in J-N.

was evident from E11.5 and often became severe by E12.5. Microscopic examination of paraffin-embedded and Hematoxylin and Eosin (HE)-stained sections confirmed the macroscopic findings (Fig. 2D-G). In addition, $LRP1^{rec/rec}$ embryos showed anasarca and their cardinal veins and jugular veins appeared distended. In summary, this morphology was compatible with extensive hemorrhage and secondary circulatory failure leading ultimately to the death of the embryos.

Further investigation into the cause of the profuse bleeding in *Lrp1*-deficient embryos revealed an underlying vascular defect. On microscopic examination, compared with wild-type embryos (Fig. 2H,J), the aorta in *Lrp1*-deficient embryos was grossly dilated with a thin and disorganized smooth muscle cell layer (Fig. 2I,K). Areas of interrupted endothelial integrity could be identified where bleeding into the perivascular soft tissue had occurred (Fig. 2L). Immunohistochemical analysis with an anti-desmin antibody confirmed the absence of an organized tunica media in the *Lrp1*-deficient embryos (Fig. 2N) as compared with LRP1-containing embryos (Fig. 2M). Examination of sections from wild-type embryos with antibodies directed against LRP1 and smooth muscle actin (SMA) revealed that LRP1 is abundantly expressed in aortic smooth muscle cells (Fig. 3A, upper panels), whereas only very little LRP1 could be detected in the aortic endothelium by co-staining with anti-LRP1 and anti-CD31 (also known as PECAM1) as an endothelial marker (Fig. 3D). The thickness of the aortic wall was quantified after staining of sections from *Lrp1*-deficient and LRP1-containing control embryos with an anti-SMA antibody (Fig. 3B,C). Comparison of both the number of smooth muscle cell layers (Fig. 3Ca,c) and the media thickness (Fig. 3Cb,d) revealed no significant difference between *Lrp1*-deficient and control embryos at E11.5. At E12.5, however, a significantly thinner tunica media was noted in the absence of LRP1.

On further examination, an additional defect of small vessel architecture was identified. Electron microscopy images of capillaries in the brain of E12.5 animals showed that, in the absence of LRP1, pericytes are missing (Fig. 4Ab-d), whereas they are easily identified by their characteristic processes and location within the endothelial basement membrane in the presence of LRP1 (Fig. 4Aa). Examination by confocal microscopy after staining with antibodies directed against the pericyte marker PDGFRβ and the endothelial marker CD31 revealed the almost complete absence of PDGFRβ-positive and CD31-negative pericytes in the *Lrp1*-deficient animals (Fig. 4Ba, quantification in Fig. 4Bb). Similar results were obtained after immunostaining for SMA as a pericyte marker (supplementary material Fig. S1). At E11.5, the number of putative pericytes was still low in both the *Lrp1*-deficient and in control animals. Immunohistochemical analysis with anti-LRP1 showed expression of LRP1 in capillary vessels, both in pericytes and in endothelial cells (Fig. 4Bc).

Taken together, *Lrp1*-deficient embryos apparently fail to recruit (or maintain) mural cells, i.e. pericytes and vascular smooth muscle cells, to developing vessels of different sizes.

In addition to the vascular developmental defects, the developmental delay of several other structures was observed, which possibly occurred secondary to the circulatory failure (supplementary material Fig. S2A,B). Nevertheless, somite number and crown-rump length at E11.5 and E12.5, respectively, did not show a significant difference between *Lrp1*-deficient and control embryos (supplementary material Fig. S2C).

LRP1 modulates the crosstalk between S1P and PDGF-BB pathways in migrating mesenchymal cells

Collectively, the alterations observed in the $Lrp1^{-/-}$ embryos resembled those described for mice with defective S1P signaling, i.e. those genetically engineered for homozygous loss of the S1P receptor $S1P_1$ (Liu et al., 2000). The homozygous $S1P_1$ defect is lethal by E14.5, and affected embryos show signs of defective sheathing of developing blood vessels with mural cells, resulting in hemorrhage and subsequent circulatory failure with widespread edema.

Owing to this similarity in phenotypes we examined whether S1P signaling was altered in the absence of LRP1. Expression of S1P receptors $S1P_1$ and $S1P_2$ was essentially the same in aortic and capillary endothelial cells and in the underlying aortic media of

Development (2014) 141, 4513-4525 doi:10.1242/dev.109124

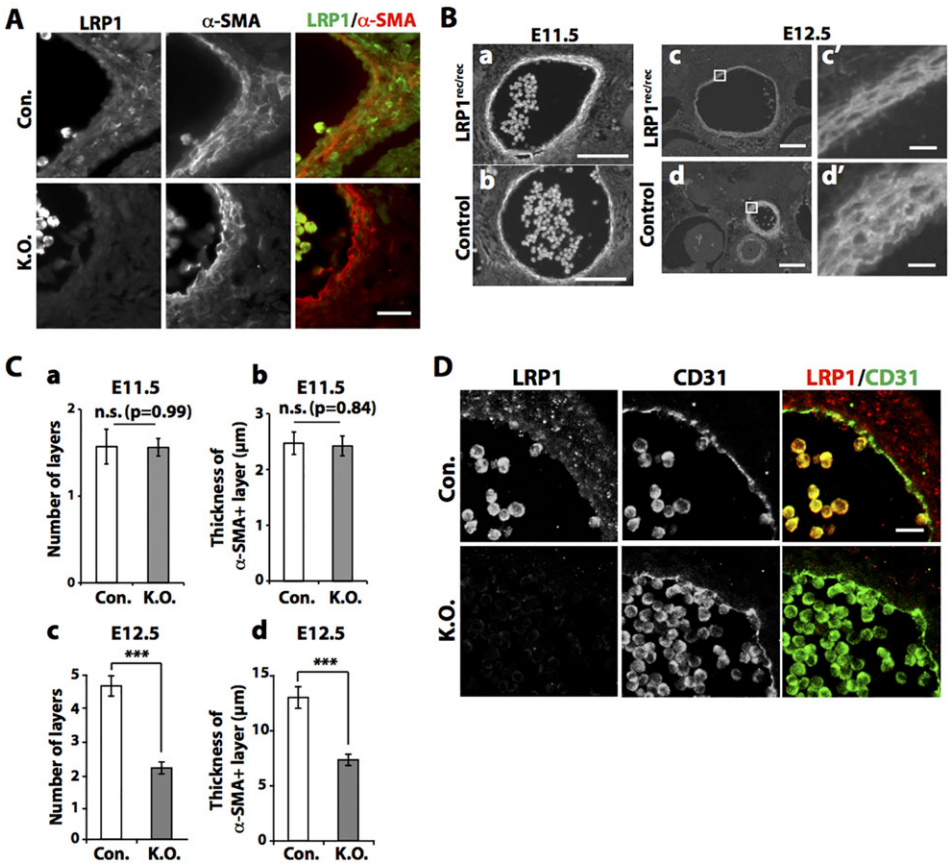

Fig. 3. LRP1 is expressed in the vascular wall, and in *Lrp1*-deficient embryos the thickness of the aortic media is reduced. (A) Transverse sections from the thoracic area of E12.5 *Lrp1*-deficient ($LRP1^{rec/rec}$) and control ($LRP1^{lox/lox}$) embryos were immunostained with anti-LRP1 (green) and anti-SMA (red) antibodies and micrographs were taken of the dorsal aortic wall. (B) Dorsal aorta of E11.5 and E12.5 *Lrp1*-deficient ($LRP1^{rec/rec}$) (a,c) and control ($LRP1^{lox/lox}$) (b,d) embryos after staining with anti-SMA (white). The boxed regions in c and d are enlarged in c′ and d′. (C) Quantitative analysis of aortic media thickness of E11.5 and E12.5 *Lrp1*-deficient ($LRP1^{rec/rec}$) and control ($LRP1^{lox/lox}$) embryos was performed from four randomly chosen regions of the anti-SMA-stained transverse aortic section by determining (a,c) the number of smooth muscle cell layers and (b,d) the breadth of the aortic media. This analysis was undertaken for three animals of each genotype. Error bars represent mean±s.e.m. ***P<0.0001; Student's t-test. (D) Transverse sections from the thoracic area of E12.5 *Lrp1*-deficient (K.O.: $LRP1^{rec/rec}$) and control (Con.: $LRP1^{lox/lox}$) embryos were immunostained with anti-LRP1 (red) and anti-CD31 (green) antibodies. Scale bars: 20 μm in A,D; 100 μm in Ba-d; 10 μm in Bc′,d′.

Lrp1-deficient and control embryos at E11.5 (supplementary material Fig. S3A-D). Subsequently, at E12.5, when hemorrhage was already evident, both $S1P_1$ and $S1P_2$ were lost from the aortic endothelium (supplementary material Fig. S3A,C). As this could not explain the vascular defects in the absence of LRP1, we examined S1P downstream signaling events in the absence and presence of LRP1. Migration of *Lrp1*-deficient and wild-type murine embryonic fibroblasts (MEFs) was studied in a transwell assay, both in the basal state and after treatment with S1P, PDGF-BB or co-treatment with both factors. The *Lrp1*-deficient cells showed increased migration compared with their wild-type counterparts in the basal state (Fig. 5A,C). Treatment with S1P did not significantly alter motility of either cell line and treatment with PDGF-BB comparably induced migration of both *Lrp1*-deficient and wild-type cells. If both PDGF-BB and S1P were applied, S1P significantly reduced PDGF-BB-induced cell motility in the wild-type cells. By contrast, in LRP1-deficient cells S1P did not significantly alter PDGF-BB-induced migration (Fig. 5B,C). To rule out underlying LRP1-independent clonal differences in the cell lines, we repeated the migration assay with *Lrp1*-deficient cells stably retransfected with either an LRP1 expression vector or with the empty plasmid backbone. Again, in the presence of LRP1, S1P significantly inhibited the PDGF-BB-dependent induction of cell migration, whereas it did not in the absence of LRP1 (Fig. 5D).

The LRP1 intracellular domain mediates modulation of S1P–PDGF-BB crosstalk

Interestingly, retransfection of the LRP1 intracellular domain was sufficient to restore the S1P effect on PDGF-BB-induced cell migration (Fig. 5D,E), indicating that modulation of cytoplasmic signaling events, rather than extracellular binding of either ligand, underlies the regulatory role of LRP1. When cells were retransfected with an expression plasmid for an LRP1 intracellular domain in which the two NPxY protein interaction motifs had been mutated, S1P did not reduce PDGF-BB-induced cell motility (Fig. 5E). This finding further corroborates the role of the LRP1 intracellular domain and its interaction with cytoplasmic scaffolding and signaling molecules in proper S1P action.

S1P downregulates PDGF-BB-induced cell migration via activation of $S1P_2$-dependent pathways in LRP1-containing cells

S1P regulates the migratory activity of mesenchymal cells primarily through its G protein-coupled receptors $S1P_1$ and $S1P_2$ (Okamoto et al., 2000; Hobson et al., 2001; Kluk and Hla, 2001; Goparaju et al., 2005; Mizugishi et al., 2005). Signaling via $S1P_1$ involves the activation of RAC1 via Gi and stimulates migration (Hobson et al., 2001; Kluk and Hla, 2001), whereas activation of $S1P_2$ via Gq and G12/13 leads to an increase in RHOA activity with a concomitant reduction in RAC1 activation and reduction in cell migration (Okamoto et al., 2000; Goparaju et al., 2005; Mizugishi et al., 2005). To test whether, in our experimental system, the inhibitory effect exerted by S1P on PDGF-BB-induced cell migration in LRP1-containing cells is mediated by $S1P_2$ as previously described, we pre-treated cells with the $S1P_2$ antagonist JTE-013. As expected, treatment with S1P no longer reduced PDGF-BB-induced cell migration in LRP1-expressing cells after blockade of $S1P_2$. Instead, S1P induced further migration under these conditions, presumably by activating $S1P_1$. In LRP1-deficient cells, where S1P did not alter PDGF-BB-induced cell migration, pre-treatment with JTE-013 had no effect on the number of migrating cells after co-stimulation with S1P and PDGF-BB (Fig. 6A). To further elucidate why S1P cannot

Development (2014) 141, 4513-4525 doi:10.1242/dev.109124

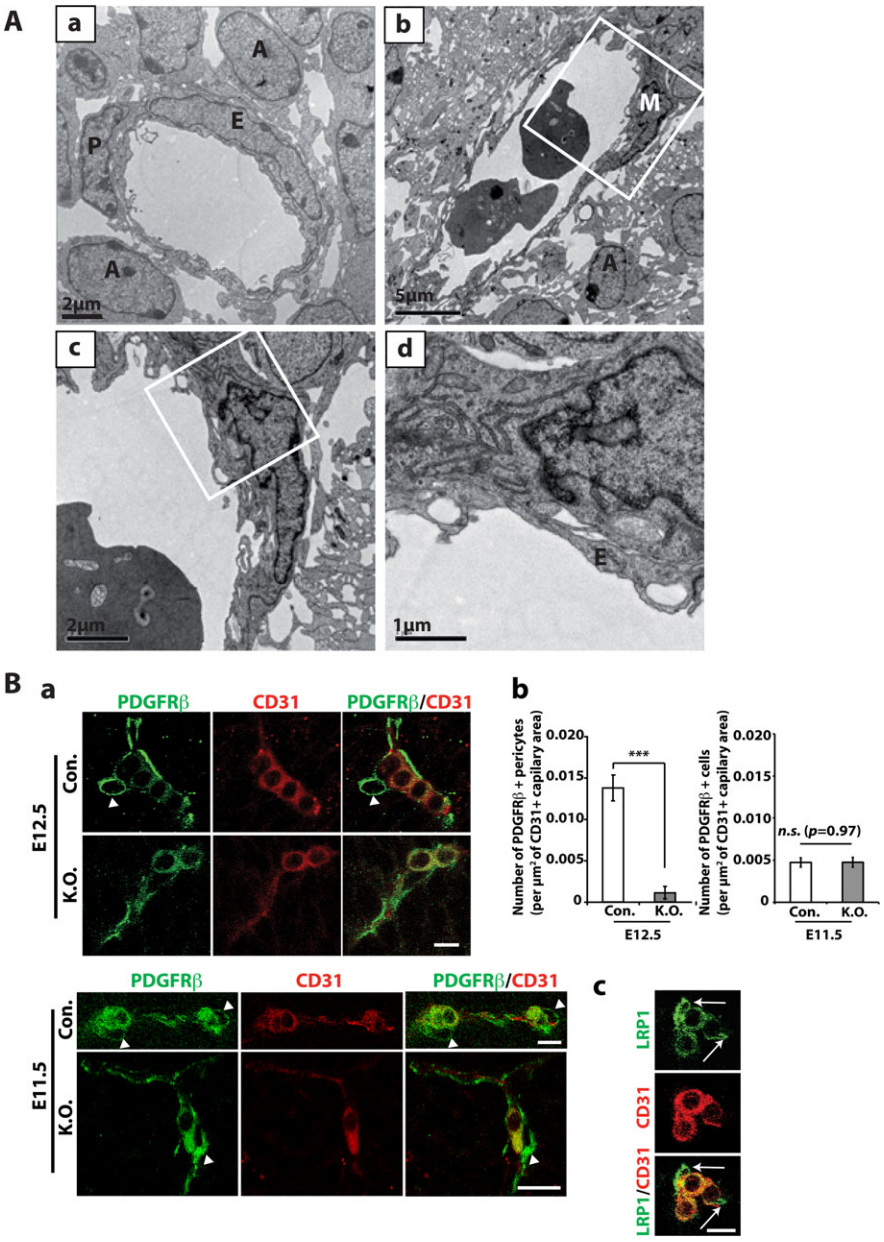

Fig. 4. Defective investment with mural cells of the developing vasculature in *Lrp1*-deficient embryos. (A) Electron micrographs of a brain capillary of E12.5 wild-type (a) or *Lrp1*$^{-/-}$ (b) embryo. The boxed regions in b and c are enlarged in c and d, respectively. A, astrocyte; E, endothelial cell; M, microglia; P, pericyte. (B) (a) Capillaries in the telencephalon of E11.5 and E12.5 *Lrp1*-deficient (MeoxCre-LRP1$^{lox/rec}$) and control (LRP1$^{lox/lox}$) embryos were analyzed after immunostaining for the pericyte marker PDGFRβ (green) and the endothelial cell marker CD31 (red). Arrowheads indicate pericytes. (b) Pericyte density of E12.5 and E11.5 *Lrp1*-deficient (MeoxCre-LRP1$^{lox/rec}$) and control (LRP1$^{lox/lox}$) embryos was determined by counting the number of PDGFRβ-positive, CD31-negative cells per area of CD31-positive capillaries (μm^2). Five random frames per animal were analyzed in four (E12.5) or three (E11.5) different mice of each genotype. At E11.5, the number of PDGFRβ-positive cells per area of CD31-positive capillaries (μm^2) was calculated from *Lrp1*-deficient and control embryos. Error bars represent mean±s.e.m. ***P<0.0001; n.s., not significant; Student's t-test. (c) Capillaries in the telencephalon of E12.5 *Lrp1*-deficient (MeoxCre-LRP1$^{lox/rec}$) and control (LRP1$^{lox/lox}$) embryos were analyzed after immunostaining for LRP1 (green) and the endothelial cell marker CD31 (red). Arrows indicate LRP1 expressed on CD31-negative mural cells, which are typically situated for pericytes on the outer side of the capillary wall. Scale bars in B: 10 μm.

inhibit PDGF-BB-induced cell migration via S1P$_2$ in LRP1-deficient cells, we compared the expression levels of *S1P$_1$* and *S1P$_2$* mRNAs in both LRP1-containing and LRP1-deficient cells by quantitative RT-PCR. The mRNAs of both receptors were equally abundant in the two cell lines (Fig. 6B). In addition, neither S1P$_1$ nor S1P$_2$ directly interacted with LRP1 in co-immunoprecipitation experiments (supplementary material Fig. S4).

We next examined activation of the S1P$_2$ downstream effector RHOA in the two cell lines after treatment with S1P and S1P/PDGF-BB co-treatment. In both LRP1-containing and LRP1-deficient cells, exposure to S1P led to comparable RHOA activation (Fig. 6C), indicating that this part of the S1P$_2$ signaling pathway is intact in the absence of LRP1.

G1-mediated S1P signaling pathways are overactive in LRP1-deficient cells

We next examined RAC1 activity after PDGF-BB and S1P/PDGF-BB co-treatment in LRP1-containing and LRP1-deficient cells. In the former, S1P/PDGF-BB co-treatment led to a significant reduction in RAC1 activity compared with PDFG-BB-induced RAC1 activity. This S1P-induced decrease in RAC1 activity did not occur in the LRP1-deficient cells (Fig. 6D). In the context of cell migration, RAC1 is regulated by S1P via S1P$_2$, leading to a reduction in RAC1 activity, and via S1P$_1$ and activation of the heterotrimeric Gi protein, resulting in an increase in RAC1 activity (Hobson et al., 2001; Goparaju et al., 2005). To test whether the failure to constrain RAC1 activity was due to increased activation of S1P$_1$ in LRP1-deficient cells, we employed the selective S1P$_1$ antagonist W146 in the transwell migration assays. Pre-treatment with W146, however, did not alter the migratory behavior of LRP1-containing or LRP1-deficient cells, indicating that the dysregulation of migration in the LRP1-deficient cells does not occur at the S1P$_1$ receptor level (Fig. 7B). We therefore tested whether downstream inhibition of Gi by pertussis toxin would restore the inhibitory effect of S1P in the LRP1-deficient cells. Pre-treatment with pertussis toxin augmented the inhibitory effect of S1P on cell migration in both LRP1-containing and LRP1-deficient cells, such that

Development (2014) 141, 4513-4525 doi:10.1242/dev.109124

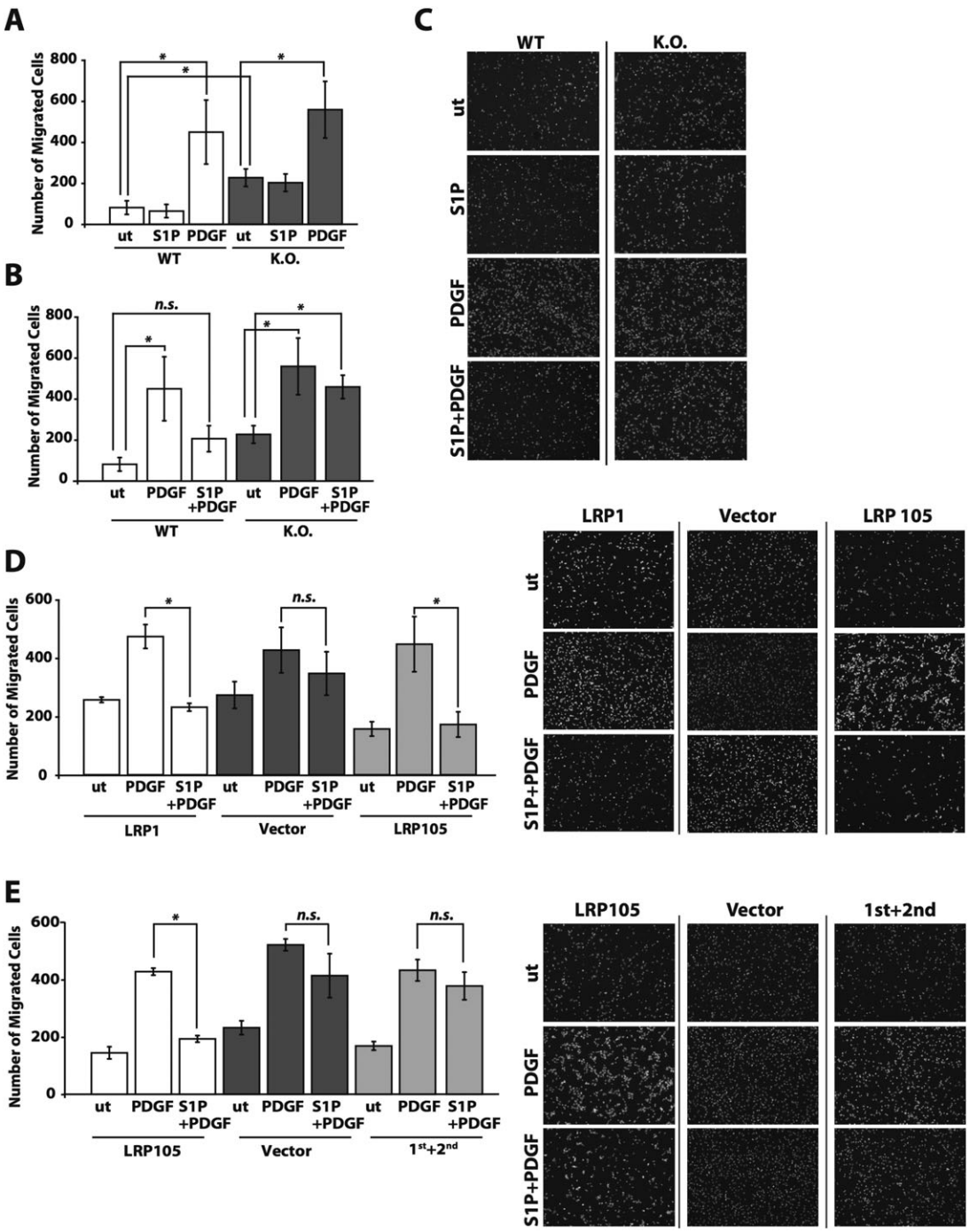

Fig. 5. Inhibition of PDGF-BB-induced cell migration by S1P is LRP1-dependent and mediated by the LRP1 intracellular domain. (A) LRP1-expressing (WT) and *Lrp1*-deficient (K.O.) fibroblasts were seeded into transwells of 8 µm pore size, allowed to settle for 1 h and then to migrate through the membrane for 5 h towards an S1P gradient, a PDGF-BB gradient or no gradient. (B) As in A, using the following gradients: an S1P+PDGF-BB gradient, a PDGF-BB gradient or no gradient. (C) Representative images (from experiments in A and B) of cells that have migrated through the transwell membrane. (D) *Lrp1*-deficient cells stably retransfected with an LRP1 expression plasmid (LRP1), with the empty plasmid vector (Vector) or an expression plasmid for the LRP1 intracellular domain (LRP105) were seeded into transwells and allowed to migrate toward an S1P+PDGF-BB gradient, a PDGF-BB gradient or no gradient. (E) *Lrp1*-deficient cells stably retransfected with LRP105, empty plasmid vector, or an expression plasmid for the LRP1 intracellular domain in which the two NPxY motifs have been mutated to AAAA (1^{st}+2^{nd}) were seeded into transwells and allowed to migrate toward an S1P+PDGF-BB gradient, a PDGF-BB gradient or no gradient. ut, untransfected controls. In each case, *N*=3 independent experiments (each performed in duplicate). Error bars indicate s.e.m. **P*<0.05; n.s., not significant; Student's *t*-test.

single treatment with S1P led to a reduction in cell migration. The inhibitory effect on PDGF-BB-induced cell migration was enhanced in LRP1-containing cells and, in addition, was restored in LRP1-deficient cells (Fig. 7A), indicating that overactive Gi-mediated signaling prevented the S1P inhibitory effect in non-pertussis toxin-treated LRP1-deficient cells. Similar results were obtained when RAC1 activity was measured in LRP1-deficient versus LRP1-containing cells. Treatment with S1P in addition to PDGF-BB

Development (2014) 141, 4513-4525 doi:10.1242/dev.109124

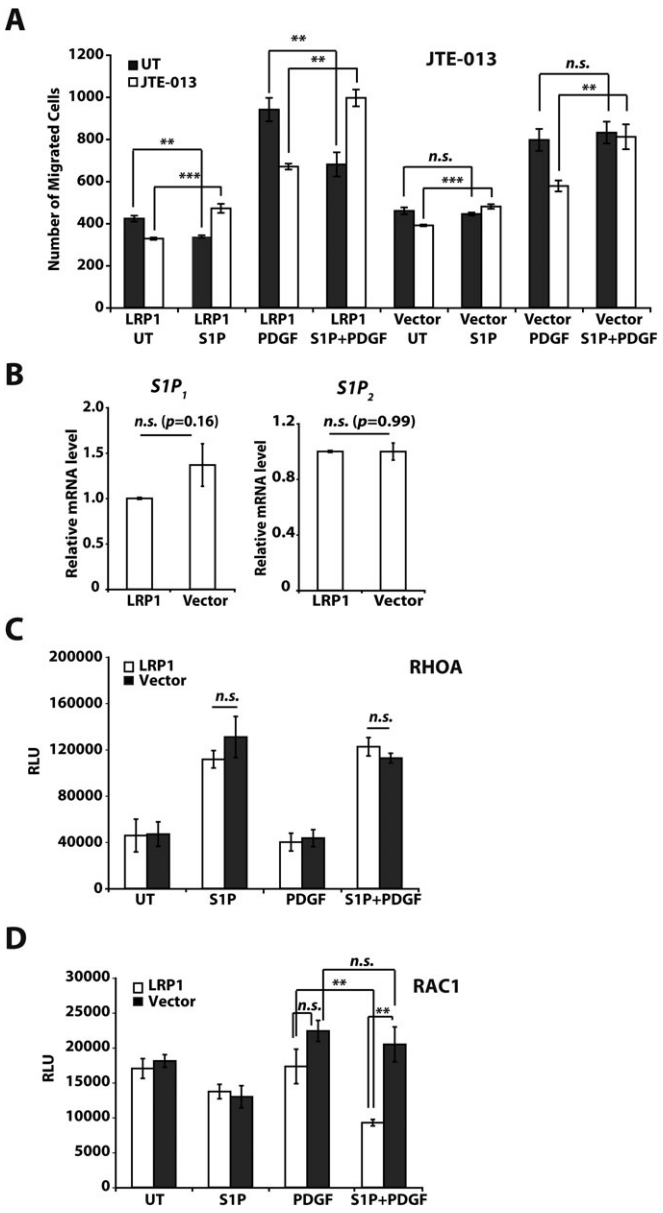

Fig. 6. The LRP1-dependent inhibition of PDGF-BB-induced cell migration by S1P is mediated by $S1P_2$ via RHOA activation and RAC1 inhibition, the latter being defective in the absence of LRP1. (A) *Lrp1*-deficient cells stably retransfected with an LRP1 expression plasmid (LRP1) or with the empty plasmid vector (Vector) were seeded into transwells and allowed to migrate toward an S1P gradient, an S1P+PDGF-BB gradient, a PDGF-BB gradient or no gradient after pretreatment for 20 min with the $S1P_2$ antagonist JTE-013 (10 μM) or pretreatment with the vehicle alone. (B) Relative expression of $S1P_1$ and $S1P_2$ mRNA in *Lrp1*-deficient cells stably retransfected with an LRP1 expression plasmid or with the empty plasmid vector. (C,D) *Lrp1*-deficient cells stably retransfected with an LRP1 expression plasmid or with the empty plasmid vector were treated with 1 μM S1P and/or 50 ng/ml PDGF-BB or were left untreated. Active RHOA (C) or active RAC1 (D) was determined in cell lysates by a chemiluminescence-based ELISA (RLU, relative luminescence units). *N*=3 (A,C), 8 (B) or 4 (D) independent experiments (each performed in duplicate). In each case, error bars indicate s.e.m. $^{**}P<0.05$, $^{***}P<0.005$; n.s., not significant; Student's *t*-test.

reduced RAC1 activity in the presence of LRP1, but not in LRP1-deficient cells. Pretreatment with pertussis toxin restored the inhibitory effect of S1P in the absence of LRP1 (Fig. 7C). Immunocytochemical analysis of LRP1-containing and LRP1-deficient cells with an antibody against Gi-GTP confirmed an excess of activated Gi after S1P and PDGF-BB co-treatment in LRP1-deficient cells (Fig. 7D). LRP1 thus functions as an integrator of signaling input, regulating the activity of heterotrimeric Gi protein and, subsequently, that of small GTPases involved in cytoskeleton remodeling in migrating cells. Immunocytochemical analysis of the LRP1-containing MEFs showed localization of LRP1 on filopodial protrusions and on lamellipodia (Fig. 7E), where it would be correctly located to fulfill its regulatory functions during cell migration.

To examine whether LRP1 also modulates Gi-dependent integration of S1P and PDGF-BB signals in endothelial cells, we used human umbilical cord venous endothelial cells (HUVECs), which contain very little LRP1 in their native state (Fig. 8A). We compared levels of Gi-GTP before and after treatment with S1P and/or PDGF-BB in HUVECs transfected with an expression plasmid for LRP1 or with the empty plasmid vector. Transfection of LRP1 decreased basal levels of Gi-GTP in HUVECs (Fig. 8Ba,b). After treatment with S1P there was significantly more active Gi in vector-transfected control cells, whereas PDGF-BB induced comparable levels of Gi-GTP in both groups (Fig. 8Bc-f). Co-treatment with S1P significantly reduced Gi-GTP in PDGF-BB-treated HUVECs only when LRP1 was overexpressed (Fig. 8Bg,h), indicating that the molecular interaction described in fibroblasts also takes place in endothelial cells.

Similar results were obtained when SV40-transformed endothelial cells (SVEC4-10), which do express LRP1, were transfected with siRNA to silence LRP1 expression (Fig. 8C). Basal levels of Gi-GTP were higher in these cells, which was exaggerated after transfection of LRP1 siRNA. Single treatment with S1P or PDGF-BB effected little change in the already high Gi-GTP levels, whereas after S1P/PDGF-BB co-treatment Gi-GTP levels were constrained only in the presence of LRP1, and silencing of *Lrp1* led to further augmentation of Gi-GTP in SVEC4-10 cells (Fig. 8D).

In summary, our current findings show that LRP1 plays an essential role for embryonic development in the embryo proper. LRP1 is necessary for the correct investment of developing vessels with mural cells. In its absence disturbed vessel architecture leads to extensive hemorrhage and secondary circulatory failure. Our *in vitro* data indicate that LRP1-dependent modulation of S1P–PDGF-BB crosstalk, which has been shown to be crucial in the regulation of cell migration and vascular development, might underlie the essential role of LRP1 in vessel maturation. LRP1 is located on lamellipodia of mesenchymal cells and mediates integration of S1P and PDGF-BB signaling input via its intracellular domain at the level of heterotrimeric Gi protein, leading to subsequent influence on RAC1 activity and cell migration (Fig. 9).

DISCUSSION

In this study we have unveiled an unexpected role of the lipoprotein receptor LRP1 in blood vessel maturation. The developmental phenotype of LRP1-deficient mice resembles that of mice with genetic defects in S1P signaling, and our *in vitro* studies reveal a hitherto unknown function of LRP1 in modulating S1P signaling, specifically in supporting its inhibitory effect on PDGF-BB-induced cell migration via Gi-dependent regulation of Rho family GTPase activity.

LRP1 expression in extraembryonic tissues cannot rescue *Lrp1*-deficient embryos

In the *Lrp1*-deficient strain examined here, E11.5-12.5 was identified as the time of lethality of *Lrp1*-deficient embryos (Table 1). A previous study did not find viable $Lrp1^{-/-}$ embryos

Development (2014) 141, 4513-4525 doi:10.1242/dev.109124

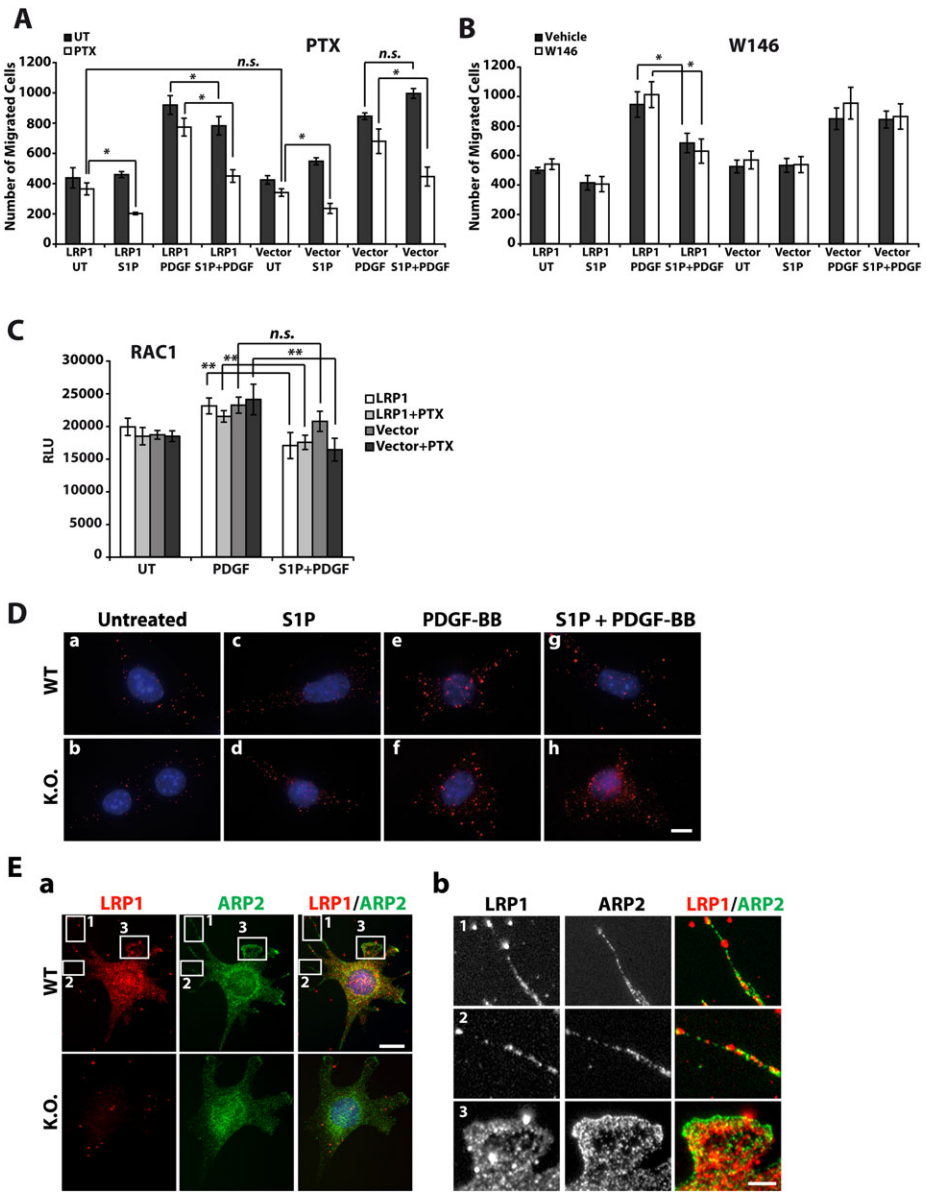

Fig. 7. LRP1 modulates S1P signaling via pertussis toxin-sensitive G proteins. (A) *Lrp1*-deficient cells stably retransfected with an LRP1 expression plasmid (LRP1) or with the empty plasmid vector (Vector) were seeded into transwells and allowed to migrate toward an S1P gradient, an S1P+PDGF-BB gradient, a PDGF-BB gradient or no gradient after pretreatment for 2 h with 200 ng/ml pertussis toxin (PTX) or with vehicle alone. (B) Cells stably transfected with LRP1 expression plasmid or empty plasmid vector were seeded into transwells and allowed to migrate toward an S1P gradient, an S1P+PDGF-BB gradient, a PDGF-BB gradient or no gradient after pretreatment for 1 h with 10 µM W146 or vehicle alone. (C) Cells stably transfected with LRP1 expression plasmid or empty plasmid vector were pretreated for 2 h with 200 ng/ml pertussis toxin or left untreated. They were then treated with 1 µM S1P and/or 50 ng/ml PDGF-BB for 1 min or were left untreated. Active RAC1 was determined in cell lysates by a chemiluminescence-based ELISA. *N*=5 (A,B) or 3 (C) independent experiments (each performed in duplicate). Error bars indicate s.e.m. **P*<0.05 (A,B) or ***P*<0.01 (C); n.s., not significant; Student's *t*-test. (D) LRP1-expressing (WT, a,c,e, g) and *Lrp1*-deficient (K.O., b,d,f,h) fibroblasts were treated with 1 µM S1P and/or 50 ng/ml PDGF-BB for 1 min or were left untreated. They were then stained with an anti-G_i-GTP antibody (red) and counterstained with DAPI. (E) (a) LRP1-expressing (WT) and *Lrp1*-deficient (K.O.) fibroblasts were stained with antibodies against LRP1 (red) and actin-related protein 2 [ARP2 (ACTR2), green]. (b) Enlargements of regions 1-3 from a. LRP1 is present on ARP2-positive filopodial protrusions (1 and 2). In lamellipodia, there is partial colocalization of ARP2 and LRP1 (in 3). Scale bars: 10 µm in D,Eb; 20 µm in Ea.

beyond E12.5, and their number was smaller than expected from E9.5 on (Herz et al., 1993). The exact nature of the genetic inactivation of *Lrp1* differed in this and our current study. It is thus conceivable that a difference exists in the genomic information that is lost in addition to the sequences coding for the LRP1 protein, e.g. information carried by non-coding RNAs. In both cases, however, loss of LRP1 was complete and differences in the time of embryonic lethality between the two strains are also likely to stem from variations in the genetic background of the lines.

The widespread expression and multifunctionality of LRP1 theoretically enable it partake in diverse developmental tasks (May et al., 2005; Lillis et al., 2008). These include a role in nutrient transport in the placenta in analogy to its LDLR gene family relative, the insect vitellogenin receptor (Barber et al., 1991), as opposed to a role in the embryo proper. Here we showed that the presence of LRP1 in the placenta and other extraembryonic tissues is not sufficient to rescue conditionally *Lrp1*-deficient animals that lack LRP1 in the embryo proper, indicating that the predominant function of LRP1 during development is in the latter. It is of note, however, that in the MeoxCre-LRP1$^{lox/lox}$ conditionally *Lrp1*-deficient embryos, where recombination takes place in epiblast-derived tissues, LRP1 is also lost in the epiblast-derived extraembryonic mesoderm, including the visceral mesoderm of the yolk sac and the allantoic and chorionic mesoderm of the chorio-allantoic placenta. Thus, a role for LRP1 in these tissues cannot be excluded, especially for the formation of the fetal part of the placental vasculature, but a predominant function as a nutrient transporter is still unlikely, as one would expect this to occur on the labyrinthine syncytiotrophoblast, which is in direct contact with maternal blood.

The slight delay in lethality in the conditionally *Lrp1*-deficient embryos might also be attributable to the incomplete recombination of the floxed *Lrp1* allele in the conditional line (Fig. 1). It was noted during the initial characterization of the Meox2Cre line in combination with a reporter strain that recombination was mosaic, occurring in 95% of cells in the embryo proper (Tallquist and Soriano, 2000).

Lrp1 deficiency in the embryo proper leads to defects in vessel maturation and subsequent circulatory failure

Morphological analysis of *Lrp1*-deficient embryos revealed that, around the great arterial vessels, the smooth muscle cell layers of

Development (2014) 141, 4513-4525 doi:10.1242/dev.109124

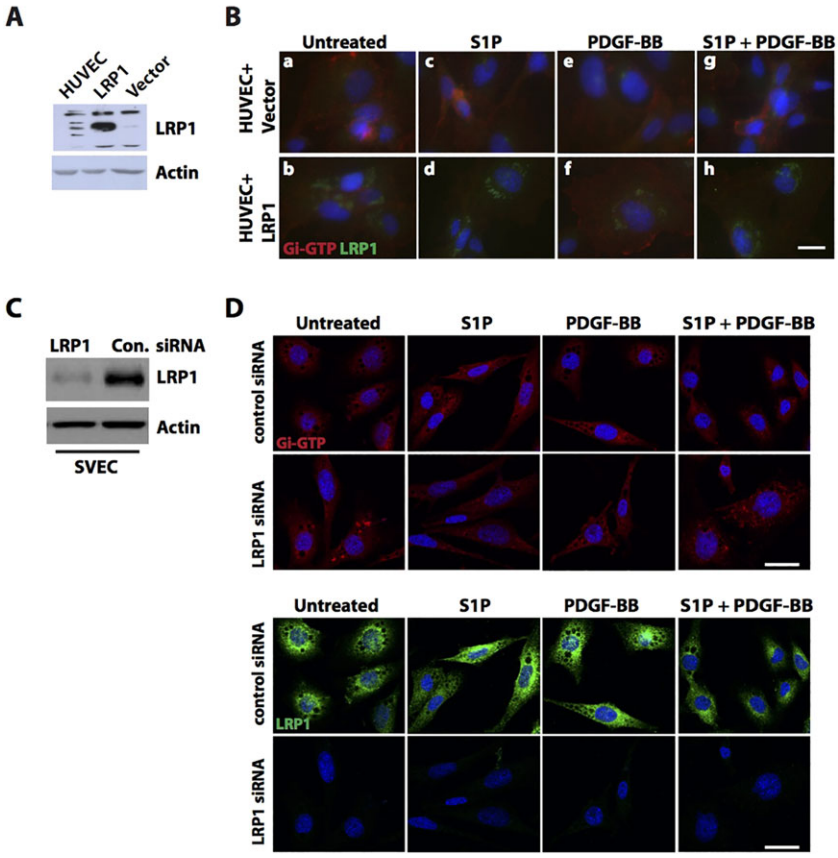

Fig. 8. LRP1 modulates S1P signaling in endothelial cells. (A) HUVECs, as well as *Lrp1*-deficient fibroblasts stably retransfected with an LRP1 expression plasmid (LRP1) or with empty plasmid vector (Vector) were cultured. Whole cell lysates were subjected to western blotting against LRP1, with actin as a loading control. (B) HUVECs transiently transfected with an LRP1 expression plasmid (HUVEC+LRP1) or with the empty plasmid vector (HUVEC +Vector) were treated with 1 µM S1P and/or with 50 ng/ml PDGF-BB for 1 min or were left untreated and G_i activation was detected by immunocytochemistry. The cells were stained for activated Gi-GTP (red) and LRP1 (green), with DAPI as counterstain. (C) SVEC4-10 cells were transfected with siRNA targeted at the mouse *Lrp1* sequence (LRP1 siRNA) or firefly luciferase sequence (control siRNA). Knockdown of LRP1 was assayed by western blotting from whole cell lysates. (D) Transiently transfected SVEC4-10 cells were treated with 1 µM S1P and/or 50 ng/ml PDGF-BB for 2 min or left untreated. The cells were immunostained for Gi-GTP (red) and LRP1 (green), with DAPI counterstain. Scale bars: 10 µm in B; 20 µm in D.

the tunica media are greatly reduced and disorganized compared with wild-type embryos (Fig. 2H-L). Additionally, electron microscopy analysis of brain capillaries showed an absence of pericytes in the *Lrp1*-deficient embryos (Fig. 4Ab-d). The initial description of conventionally engineered *Lrp1*-deficient embryos included evidence of hemorrhage (Herz et al., 1993). By contrast, genetically engineered mice that lack *Lrp1* in smooth muscle cells, including those of the vascular wall, show considerable thickening of the tunica media with an increase in smooth muscle cells (Boucher et al., 2003). This discrepancy is likely to be explained by two crucial differences in the mouse strains examined. First, to obtain mice that lack *Lrp1* in smooth muscle cells only, Cre recombinase was expressed under the control of the *Sm22* (*Tagln*) promoter (Boucher et al., 2003). Thus, recombination of *Lrp1* takes place only after differentiation of the smooth muscle lineage, whereas in our study LRP1 is already lost in the mesenchymal precursor that gives rise to both types of mural cells, i.e. pericytes and smooth muscle cells. Second, in our study LRP1 is also lacking in endothelial cells, which play a crucial role in the investment of developing vessels with mural cells (Bjarnegard et al., 2004).

Defects in the investment of blood vessels with mural cells have been described in genetically engineered mice with dysregulation of various signaling pathways (Adams and Alitalo, 2007). The crucial roles of PDGF-BB and PDGFRβ in this process have been demonstrated through analysis of knockout mice (Soriano, 1994; Lindahl et al., 1997; Tallquist et al., 2003). Both types of animals, however, die perinatally, considerably later than the *Lrp1*-deficient mice. TGFβ-deficient mice, on the other hand, suffer from defects of vasculogenesis in addition to disturbed vessel maturation and show even more profoundly disrupted development than LRP1-deficient animals, with earlier lethality (Martin et al., 1995). Interestingly, mice deficient in $S1P_1$ display a developmental phenotype that closely resembles that of the *Lrp1*-deficient animals (Liu et al., 2000). They exhibit a defect in mural cell investment of their blood vessels, which was attributed to the lack of normal crosstalk between S1P and PDGF receptor pathways (Hobson et al., 2001).

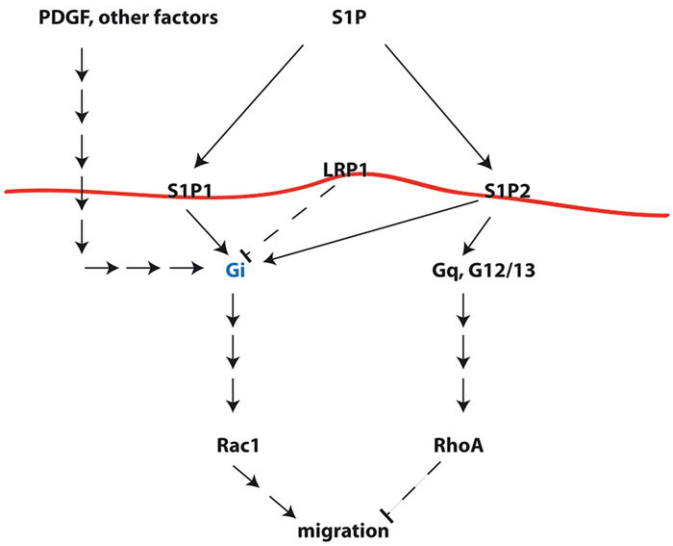

Fig. 9. Schematic model of LRP1 acting via Gi to modulate S1P–PDGF-BB crosstalk. LRP1 restrains the activation of Gi, which integrates input from several signaling pathways and mediates the promigratory effect of S1P-activated S1P1. Red line indicates the cell membrane.

Development (2014) 141, 4513-4525 doi:10.1242/dev.109124

Owing to the phenotypic similarities between *Lrp1*-deficent mice and those with a genetic defect in S1P signaling, we hypothesized that LRP1 might modulate S1P-induced cellular responses. As LRP1 is already known to interact with and regulate PDGFRβ signaling (Boucher et al., 2002; Loukinova et al., 2002), we specifically tested whether LRP1 modulates S1P–PDGF-BB crosstalk.

LRP1 is necessary for S1P to modulate PDGF-BB-induced cell migration

When migration of MEFs expressing or lacking *Lrp1* was compared, it transpired that, although PDGF-BB induced similar maximal rates of migration in both cell lines, S1P could modulate, i.e. reduce, this effect only in the presence of LRP1 (Fig. 5B). Several signaling properties of LRP1 might underlie its role in mediating the S1P effect on PDGF-BB-induced cell migration. First, LRP1 itself negatively regulates PDGFRβ-mediated signaling processes; it directly interacts with PDGF protein and regulates its internalization and degradation (Boucher et al., 2002; Loukinova et al., 2002; Takayama et al., 2005). Nevertheless, we found that *Lrp1*-expressing and *Lrp1*-deficient MEFs show comparable migration toward a PDGF-BB gradient and that both the presence of LRP1 and treatment with S1P were necessary to reduce this effect (Fig. 5). Thus, it seems more likely that LRP1 targets S1P signaling in this context. S1P has several transmembrane receptors, all of which are G protein-coupled. $S1P_1$ has the best-documented role in angiogenesis, where it is essential for vessel maturation through investment with mural cells (Allende and Proia, 2002). Endothelial cell-specific conditional ablation of $S1P_1$ expression proved that $S1P_1$ is essential in this cell type (Allende et al., 2003). No studies concerning a mural (precursor) cell-specific ablation have been published so far, so its role in this cell type is less clear. As investment with pericytes/smooth muscle cells requires their interaction with endothelial cells, such an interaction might well be essential in mural precursors, which are targets of PDGF-BB during vascular development, as well. Although it was initially shown that S1P, via the $S1P_1$ receptor, augments PGDF-BB-induced cell migration (Hobson et al., 2001), it had long been known that S1P could inhibit the PDGF-BB-induced migration of smooth muscle cells (Bornfeldt et al., 1995) and it was subsequently demonstrated that it has a dose-dependent effect on the migration of this cell type (Boguslawski et al., 2002). $S1P_2$ has been identified as a negative regulator of RAC1 activation and cell migration (Okamoto et al., 2000). It thus seems that integration of the activity of different S1P receptors, as well as other signaling input, results in the final response in terms of cell migration and mural/endothelial cell interaction during vessel maturation.

It is conceivable that the exact mechanism that results in defective mural cell coverage differs in small and large vessels, as there is a difference in LRP1 expression between these vessel types: in brain capillaries LRP1 was abundantly identified in both endothelial cells and pericytes in control embryos, whereas in the aortal endothelium there was very little LRP1 but strong LRP1 expression in the smooth muscle cell layers (Fig. 4 and Fig. 3, respectively). This could mean that LRP1 exerts its regulatory role in both endothelial cells and pericytes in capillaries, whereas in the large vessel type it seems more likely that its role is confined to cells of the smooth muscle layer.

Lack of LRP1 results in the failure of S1P to downregulate RAC1 activity in PDGF-BB-treated cells due to inadequate activity of Gi

A central player both in S1P signaling pathways and in the regulation of cell migration is the heterotrimeric G protein Gi. It receives input both from $S1P_1$, which signals mainly via Gi, and to a lesser extent from $S1P_2$, which also uses Gq and G12/13 (Daum et al., 2009). In addition, PDGF-BB has been described to signal via Gi in airway smooth muscle cells (Conway et al., 1999). Our experiments showed that in the LRP1-containing cells S1P exerts its influence on PDGF-BB-induced cell migration via $S1P_2$ (Fig. 6A). In the absence of LRP1, S1P was still able to induce RHOA activity (Fig. 6C), which has been shown to play an important role in the negative regulation of migration by S1P (Goparaju et al., 2005), although it failed to decrease PDGF-BB-induced cell migration. As it also failed to downregulate RAC1 activity (Fig. 6D), one might speculate that there is not a lack of antimigratory activity but a surplus of promigratory input in the LRP1-deficient cells. Indeed, inhibition of Gi by pertussis toxin restored the S1P-dependent decrease in PDGF-BB-induced cell migration (Fig. 7A) and RAC1 activity (Fig. 7C) in the LRP1-deficient cells. Apparently, the increased Gi activity in the LRP1-deficient cell line does not stem from a preponderance of $S1P_1$ activation by S1P, as blockade of $S1P_1$ by the antagonist W146 had no influence (Fig. 7B) on cell migration in the transwell assay. Furthermore, co-immunoprecipitation experiments did not show direct interaction of LRP1 with $S1P_1$ (nor $S1P_2$) (supplementary material Fig. S4) and expression levels of $S1P_1$ (and $S1P_2$) are comparable regardless of the presence of LRP1 (Fig. 6B; supplementary material Fig. S3). The exact molecular mechanism by which LRP1 modulates Gi activity remains to be elucidated. As we could show that LRP1 exerts its influence via its intracellular domain, with the NPxY protein interaction motifs being necessary for this activity (Fig. 5D,E), it might control the assembly of the intracellular signaling scaffold, where Gi is activated. The localization of LRP1 in lamellipodia (Fig. 7E) would suit such a role and, interestingly, LRP1 has been found to modulate signaling processes via pertussis toxin-sensitive G proteins in the context of focal adhesion disassembly (Orr et al., 2002), ApoE4-induced neuronal apoptosis (Hashimoto et al., 2000) and LRP1-dependent signaling processes in macrophages (Misra et al., 1994).

Thus, the unexpected role of LRP1 in the modulation of S1P signaling is likely to have an impact not only on vascular development, as shown here, but also on S1P action in other contexts, such as tumor angiogenesis and the pathogenesis of atherosclerosis.

MATERIALS AND METHODS

Chemicals

PDGF-BB was purchased from Sigma-Aldrich, sphingosine-1-phosphate was from Biomol, JTE-013 was from Cayman Chemical, W146 from Avanti Polar Lipids, (2-hydroxypropyl)-β-cyclodextrin from Tocris Bioscience and pertussis toxin from Biozol. W146 was solubilized in 10 mM Na_2CO_3/2% (2-hydroxypropyl)-β-cyclodextrin to provide a 5 mM stock solution.

Animals

Mice carrying a *loxP*-marked *Lrp1* allele were described previously (Rohlmann et al., 1996). To obtain epiblast-specific recombination of the floxed allele, these mice were bred to animals heterozygous for a knock-in of the viral Cre recombinase into the *Meox2* locus (Tallquist and Soriano, 2000). Embryos completely deficient for *Lrp1* were obtained by mating mice heterozygous for the recombined *Lrp1* allele derived from the MeoxCre-$LRP1^{lox}$ line ($LRP1^{lox/rec}$×$LRP1^{lox/rec}$).

Animals were kept under standard laboratory conditions. Experiments were carried out according to the principles of good laboratory animal care and were approved by the Regierungspräsidium Freiburg.

Development (2014) 141, 4513-4525 doi:10.1242/dev.109124

Preparation of organ lysates and western blot analysis

Organs were dissected from embryos as indicated in the Results section and homogenized in cold lysis buffer [PBS (pH 7.4) containing 0.5% Triton X-100 and EDTA-free protease inhibitor cocktail (Roche)]. After centrifugation (4 min, 17,000 ***g*** at 4°C) supernatants were subjected to SDS-PAGE and western blotting according to standard procedures. Preparation of membrane fractions was as described (Marschang et al., 2004). LRP1 was detected with an LRP1 antiserum directed against the C-terminus (Herz et al., 1988). After incubation with an HRP-conjugated secondary antibody, bound antibodies were visualized by enhanced chemiluminescence (ECL) using Immobilon Western Chemiluminescence HRP Substrate (Millipore).

Whole-mount *in situ* hybridization

Transcription of sense and antisense probes was performed using the DIG RNA Labeling Kit (Roche) followed by purification with Mini Quick Spin RNA columns (Roche). Whole-mount *in situ* hybridization was then performed according to Belo et al. (1997). For cloning of the *Lrp1* cDNA fragment see supplementary Methods.

Paraffin sections and immunohistochemistry

Embryos were dissected from pregnant mice at the time points indicated, fixed in 4% paraformaldehyde (PFA) overnight and embedded in paraffin according to standard procedures; 5 µm sections were cut and rehydrated for further analysis. They were either stained with Hematoxylin-Eosin or subjected to immunohistochemical analysis (IHC). For detection with primary antibodies, paraffin sections were incubated in Tris-EDTA buffer (10 mM Tris, 1 mM EDTA, 0.05% Tween 20, pH 9.0) for 20 min at 95-100°C. Then slides were washed in PBS with 0.025% Triton X-100 and blocked with 5% donkey serum and 2% BSA in PBS containing 0.1% Triton X-100 for 2 hours at room temperature. Incubation with primary antibodies was overnight at 4°C. Alexa Fluor 488- or 555-conjugated secondary antibodies diluted 1:500 were used (A-21206, A-31572, A-21202, A-31570, A-11055, A-21432, Life Technologies). Sections were mounted in ProLong Gold (Invitrogen) and images were obtained. For details of the antibodies used, detection of anti-desmin and image acquisition see supplementary Methods.

Electron microscopy

E12.5 embryos were fixed by perfusion with 0.9 % NaCl followed by 4% PFA, 0.1% glutaraldehyde and 0.2% picric acid in 0.1 M phosphate buffer (pH 7.4) and postfixed overnight after dissection. Brains were then excised and cut in 0.1 M phosphate buffer using a Vibratome. After osmication (1% OsO_4) and dehydration in a graded series of alcohols and propylene oxide the sections were embedded in flat sheets of Durcopan (Fluka). Ultrathin sections were cut on a Leica EM UC6 ultramicrotome, mounted on formvar-coated slot nickel grids, and stained with uranyl acetate and lead citrate. Analysis and documentation were performed on a Philips CM 100 electron microscope equipped with a digital camera device (Gatan, Orius SC600).

Cell culture and stable transfection of MEFs

MEFs derived from wild-type or *Lrp1*-deficient embryos were maintained in DMEM with glucose 4.5 g/l, 2 mM L-glutamine (Invitrogen), 100 U/ml penicillin, 100 µg/ml streptomycin sulfate (Invitrogen) and 8% FCS (Sigma Aldrich).

Mutant *Lrp1* plasmids and generation of stable transfectants have been described previously (Zurhove et al., 2008). In addition, mutations of the two NPxY motifs in the LRP1 cytoplasmic domain to AAAA were introduced into the cDNA by overlapping PCR using mutated primers (Zurhove et al., 2008; see supplementary Methods).

Culture and transient transfection of primary HUVECs and SVEC4-10 cells

HUVECs were cultured in Vascular Cell Basal Medium (ATCC) supplemented with Endothelial Cell Growth Kit-VEGF (ATCC) at 37°C in a 5% CO_2 atmosphere. HUVECs were transiently transfected (for details see supplementary Methods) at ~70% confluency with an *Lrp1* expression plasmid or empty vector (Zurhove et al., 2008).

SVECs were cultured in DMEM with glucose 4.5 g/l, 4 mM L-glutamine (Invitrogen) and 10% FCS (Sigma-Aldrich). Transfection with siRNA was performed with Lipofectamine 2000 (Invitrogen) according to the manufacturer's instruction (see supplementary Methods for sequence information). The cells were incubated for 48 h before further analysis.

Transwell assays

All experiments were performed in duplicate and repeated independently at least three times. Insert membranes (PET, 0.3 cm^2, 8 µm pore size; BD Falcon) were incubated with poly-D-lysine (0.05 mg/ml; Sigma) for 1 h at 37°C and subsequently with collagen I (0.01%; Sigma) overnight at 4°C. 100,000 cells per insert were seeded in DMEM (4.5 g/l glucose, 0.1% FBS) and allowed to attach for 1 h. Then, chemoattractants (1 µM S1P or 50 ng/ml PDGF-BB) were added to the lower chamber and cells were allowed to migrate through the membrane for 5 h. They were then fixed with 4% PFA, permeabilized with 0.01% Triton X-100 and stained with DAPI (1 µg/ml). Cells on the upper side of the membrane were removed using a cotton swab. Images of five random fields per insert were taken with an Olympus BX-50 fluorescence microscope. Cells were counted using ImageJ (NIH). Statistical analysis employed Student's *t*-test.

Quantitative real-time PCR

RNA was extracted from MEFs grown to 95-100% confluence with Trizol (Invitrogen) and then treated with RNase-free DNase I (Fermentas). For cDNA synthesis, random primers (Promega), M-MLV reverse transcriptase (Promega), RNase inhibitor (Promega) and dNTPs (Fermentas) were used. The real-time PCR reaction was set up with 2x Absolute QPCR SYBR Green Mix with Fluorescein (Abgene) on a single-color real-time PCR detection system (Bio-Rad MyiQ with MyiQ Optical System Software version 1.0). For primer sequences see supplementary Methods. To compare expression levels, the ΔΔCt method was used. Ct values were standardized with respect to *Gapdh*. For all experiments, samples were assayed at least in duplicate and the mean of Ct was used for further calculations. Experiments were repeated independently eight times.

G-Lisa assays

Chemiluminescence-based RAC1 (cat. #BK126) and RHOA (cat. #BK121) G-Lisa activation assays were performed according to the manufacturer's (Cytoskeleton) instructions. Briefly, 450,000 MEFs were seeded per 60 mm dish in DMEM (4.5 g/l glucose) with 0.1% FCS. After 24 h, cells were stimulated with S1P (1 µM), PDGF-BB (50 ng/ml) or both for 1 min. Then they were washed with ice-cold PBS and lysed using the lysis buffer provided with the kit. After adjustment to a protein concentration of 1 mg/ml, the luminescence of lysates was measured with a FLUOstar OPTIMA plate reader (BMG Labtech) with 100 ms integration time.

Immunocytochemistry

MEFs, HUVECs or SVEC4-10 cells cultured on glass cover slips were fixed with 4% PFA, permeabilized and blocked with 5% donkey serum and 1% albumin in PBS containing 0.1% Triton X-100. Incubation with primary antibodies was overnight at 4°C: anti-LRP1 monoclonal antibody (50 µg/ml; Calbiochem, 438192) or affinity purified LRP1 antiserum directed against the C-terminus; rat anti-ARP2 (1:500; Abcam, ab47654); anti-active Gαi GTP monoclonal antibody (1:100; New East Biosciences, 26901). Alexa Fluor 555- or 488-labeled secondary antibodies (Invitrogen) were used at 1:1000. Nuclear counterstaining was performed with DAPI (0.1 µg/ml). Cover slips were mounted in aqueous mounting medium (Thermo Scientific) and examined with a Zeiss Axioplan 2 imaging microscope with ApoTome or Leica TCS SP5.

Acknowledgements

We thank Dr A. Horst (UKE Hamburg, Germany) for the generous provision of SVEC4-10 cells; and Aileen Koch, Barbara Joch, Jonathan Göldner and Anna Schöttler for excellent technical assistance.

Competing interests
The authors declare no competing financial interests.

Author contributions
P.M. conceived the study. C.N., P.H., S.M.G., K.Z., G.A. and P.M. designed the experiments. G.A. performed electron microscopy. C.N., P.H. and S.M.G. performed all other experiments. All authors analyzed the data. C.N., H.H.B., J.H., M.F. and P.M. wrote the manuscript.

Funding
This work was supported by the Deutsche Forschungsgemeinschaft (DFG) [Emmy Noether fellowship MA-2410/1-2,3,4 to P.M.], by the Bundesministerium für Bildung und Forschung (BMBF) [*e:bio*, FKZ0316174 to H.H.B.] and by the Humboldt Foundation (Wolfgang Paul Award to J.H.). J.H. received grants from the National Institutes of Health (NIH) [HL20948, HL63762, RCINS068697]. C.N. is a Focus Program Translational Neuroscience (FTN) fellow. M.F. is Senior Research Professor of the Hertie Foundation. Deposited in PMC for release after 12 months.

Supplementary material
Supplementary material available online at
http://dev.biologists.org/lookup/suppl/doi:10.1242/dev.109124/-/DC1

References

Adams, R. H. and Alitalo, K. (2007). Molecular regulation of angiogenesis and lymphangiogenesis. *Nat. Rev. Mol. Cell Biol.* **8**, 464-478.
Allende, M. L. and Proia, R. L. (2002). Sphingosine-1-phosphate receptors and the development of the vascular system. *Biochim. Biophys. Acta* **1582**, 222-227.
Allende, M. L., Yamashita, T. and Proia, R. L. (2003). G-protein-coupled receptor S1P1 acts within endothelial cells to regulate vascular maturation. *Blood* **102**, 3665-3667.
Barber, D. L., Sanders, E. J., Aebersold, R. and Schneider, W. J. (1991). The receptor for yolk lipoprotein deposition in the chicken oocyte. *J. Biol. Chem.* **266**, 18761-18770.
Belo, J. A., Bouwmeester, T., Leyns, L., Kertesz, N., Gallo, M., Follettie, M. and De Robertis, E. M. (1997). Cerberus-like is a secreted factor with neutralizing activity expressed in the anterior primitive endoderm of the mouse gastrula. *Mech. Dev.* **68**, 45-57.
Bjarnegard, M., Enge, M., Norlin, J., Gustafsdottir, S., Fredriksson, S., Abramsson, A., Takemoto, M., Gustafsson, E., Fässler, R. and Betsholtz, C. (2004). Endothelium-specific ablation of PDGFB leads to pericyte loss and glomerular, cardiac and placental abnormalities. *Development* **131**, 1847-1857.
Boguslawski, G., Grogg, J. R., Welch, Z., Ciechanowicz, S., Sliva, D., Kovala, A. T., McGlynn, P., Brindley, D. N., Rhoades, R. A. and English, D. (2002). Migration of vascular smooth muscle cells induced by sphingosine 1-phosphate and related lipids: potential role in the angiogenic response. *Exp. Cell Res.* **274**, 264-274.
Bornfeldt, K. E., Graves, L. M., Raines, E. W., Igarashi, Y., Wayman, G., Yamamura, S., Yatomi, Y., Sidhu, J. S., Krebs, E. G., Hakomori, S. et al. (1995). Sphingosine-1-phosphate inhibits PDGF-induced chemotaxis of human arterial smooth muscle cells: spatial and temporal modulation of PDGF chemotactic signal transduction. *J. Cell Biol.* **130**, 193-206.
Boucher, P., Liu, P., Gotthardt, M., Hiesberger, T., Anderson, R. G. W. and Herz, J. (2002). Platelet-derived growth factor mediates tyrosine phosphorylation of the cytoplasmic domain of the low Density lipoprotein receptor-related protein in caveolae. *J. Biol. Chem.* **277**, 15507-15513.
Boucher, P., Gotthardt, M., Li, W.-P., Anderson, R. G. W. and Herz, J. (2003). LRP: role in vascular wall integrity and protection from atherosclerosis. *Science* **300**, 329-332.
Boucher, P., Li, W.-P., Matz, R. L., Takayama, Y., Auwerx, J., Anderson, R. G.W. and Herz, J. (2007). LRP1 functions as an atheroprotective integrator of TGFbeta and PDFG signals in the vascular wall: implications for Marfan syndrome. *PLoS ONE* **2**, e448.
Conway, A.-M., Rakhit, S., Pyne, S. and Pyne, N. J. (1999). Platelet-derived-growth-factor stimulation of the p42/p44 mitogen-activated protein kinase pathway in airway smooth muscle: role of pertussis-toxin-sensitive G-proteins, c-Src tyrosine kinases and phosphoinositide 3-kinase. *Biochem. J.* **337**, 171-177.
Daum, G., Grabski, A. and Reidy, M. A. (2009). Sphingosine 1-phosphate: a regulator of arterial lesions. *Arterioscler. Thromb. Vasc. Biol.* **29**, 1439-1443.
Fears, C. Y., Grammer, J. R., Stewart, J. E., Jr, Annis, D. S., Mosher, D. F., Bornstein, P. and Gladson, C. L. (2005). Low-density lipoprotein receptor-related protein contributes to the antiangiogenic activity of thrombospondin-2 in a murine glioma model. *Cancer Res.* **65**, 9338-9346.
Gaengel, K., Genove, G., Armulik, A. and Betsholtz, C. (2009). Endothelial-mural cell signaling in vascular development and angiogenesis. *Arterioscler. Thromb. Vasc. Biol.* **29**, 630-638.
Goparaju, S. K., Jolly, P. S., Watterson, K. R., Bektas, M., Alvarez, S., Sarkar, S., Mel, L., Ishii, I., Chun, J., Milstien, S. et al. (2005). The S1P2 receptor negatively regulates platelet-derived growth factor-induced motility and proliferation. *Mol. Cell. Biol.* **25**, 4237-4249.
Hashimoto, Y., Jiang, H., Niikura, T., Ito, Y., Hagiwara, A., Umezawa, K., Abe, Y., Murayama, Y. and Nishimoto, I. (2000). Neuronal apoptosis by apolipoprotein E4 through low-density lipoprotein receptor-related protein and heterotrimeric GTPases. *J. Neurosci.* **20**, 8401-8409.
Hellstrom, M., Kalen, M., Lindahl, P., Abramsson, A. and Betsholtz, C. (1999). Role of PDGF-B and PDGFR-beta in recruitment of vascular smooth muscle cells and pericytes during embryonic blood vessel formation in the mouse. *Development* **126**, 3047-3055.
Herz, J., Hamann, U., Rogne, S., Myklebost, O., Gausepohl, H. and Stanley, K. K. (1988). Surface location and high affinity for calcium of a 500-kd liver membrane protein closely related to the LDL-receptor suggest a physiological role as lipoprotein receptor. *EMBO J.* **7**, 4119-4127.
Herz, J., Clouthier, D. E. and Hammer, R. E. (1992). LDL receptor-related protein internalizes and degrades uPA-PAI-1 complexes and is essential for embryo implantation. *Cell* **71**, 411-421.
Herz, J., Couthier, D. E. and Hammer, R. E. (1993). Correction: LDL receptor-related protein internalizes and degrades uPA-PAI-1 complexes and is essential for embryo implantation. *Cell* **73**, 428.
Hobson, J. P., Rosenfeldt, H. M., Barak, L. S., Olivera, A., Poulton, S., Caron, M. G., Milstien, S. and Spiegel, S. (2001). Role of the sphingosine-1-phosphate receptor EDG-1 in PDGF-induced cell motility. *Science* **291**, 1800-1803.
Kluk, M. J. and Hla, T. (2001). Role of the sphingosine 1-phosphate receptor EDG-1 in vascular smooth muscle cell proliferation and migration. *Circ. Res.* **89**, 496-502.
Kluk, M. J. and Hla, T. (2002). Signaling of sphingosine-1-phosphate via the S1P/EDG-family of G-protein-coupled receptors. *Biochim. Biophys. Acta* **1582**, 72-80.
Lillis, A. P., Van Duyn, L. B., Murphy-Ullrich, J. E. and Strickland, D. K. (2008). LDL receptor-related protein 1: unique tissue-specific functions revealed by selective gene knockout studies. *Physiol. Rev.* **88**, 887-918.
Lindahl, P., Johansson, B. R., Levéen, P. and Betsholtz, C. (1997). Pericyte loss and microaneurysm formation in PDGF-B-deficient mice. *Science* **277**, 242-245.
Liu, Y., Wada, R., Yamashita, T., Mi, Y., Deng, C.-X., Hobson, J. P., Rosenfeldt, H. M., Nava, V. E., Chae, S.-S., Lee, M.-J. et al. (2000). Edg-1, the G protein-coupled receptor for sphingosine-1-phosphate, is essential for vascular maturation. *J. Clin. Invest.* **106**, 951-961.
Loukinova, E., Ranganathan, S., Kuznetsov, S., Gorlatova, N., Migliorini, M. M., Loukinov, D., Ulery, P. G., Mikhailenko, I., Lawrence, D. A. and Strickland, D. K. (2002). Platelet-derived growth factor (PDGF)-induced tyrosine phosphorylation of the low density lipoprotein receptor-related protein (LRP). Evidence for integrated co-receptor function between LRP and the PDGF. *J. Biol. Chem.* **277**, 15499-15506.
Marschang, P., Brich, J., Weeber, E. J., Sweatt, J. D., Shelton, J. M., Richardson, J. A., Hammer, R. E. and Herz, J. (2004). Normal development and fertility of knockout mice lacking the tumor suppressor gene LRP1b suggest functional compensation by LRP1. *Mol. Cell. Biol.* **24**, 3782-3793.
Martin, J. S., Dickson, M. C., Cousins, F. M., Kulkarni, A. B., Karlsson, S. and Akhurst, R. J. (1995). Analysis of homozygous TGF beta 1 null mouse embryos demonstrates defects in yolk sac vasculogenesis and hematopoiesis. *Ann. N Y Acad. Sci.* **752**, 300-308.
Masson, O., Chavey, C., Dray, C., Meulle, A., Daviaud, D., Quilliot, D., Muller, C., Valet, P. and Liaudet-Coopman, E. (2009). LRP1 receptor controls adipogenesis and is up-regulated in human and mouse obese adipose tissue. *PLoS ONE* **4**, e7422.
May, P., Bock, H. H., Nimpf, J. and Herz, J. (2003). Differential glycosylation regulates processing of lipoprotein receptors by gamma-secretase. *J. Biol. Chem.* **278**, 37386-37392.
May, P., Herz, J. and Bock, H. H. (2005). Molecular mechanisms of lipoprotein receptor signalling. *Cell. Mol. Life Sci.* **62**, 2325-2338.
Misra, U. K., Chu, C. T., Gawdi, G. and Pizzo, S. V. (1994). The relationship between low density lipoprotein-related protein/alpha 2-macroglobulin (alpha 2M) receptors and the newly described alpha 2M signaling receptor. *J. Biol. Chem.* **269**, 18303-18306.
Mizugishi, K., Yamashita, T., Olivera, A., Miller, G. F., Spiegel, S. and Proia, R. L. (2005). Essential role for sphingosine kinases in neural and vascular development. *Mol. Cell. Biol.* **25**, 11113-11121.
Nakajima, C., Kulik, A., Frotscher, M., Herz, J., Schäfer, M., Bock, H. H. and May, P. (2013). Low density lipoprotein receptor-related protein 1 (LRP1) modulates N-methyl-D-aspartate (NMDA) receptor-dependent intracellular signaling and NMDA-induced regulation of postsynaptic protein complexes. *J. Biol. Chem* **288**, 21909-21923.
Okamoto, H., Takuwa, N., Yokomizo, T., Sugimoto, N., Sakurada, S., Shigematsu, H. and Takuwa, Y. (2000). Inhibitory regulation of Rac activation, membrane ruffling, and cell migration by the G protein-coupled sphingosine-1-phosphate receptor EDG5 but not EDG1 or EDG3. *Mol. Cell. Biol.* **20**, 9247-9261.
Orr, A. W., Pallero, M. A. and Murphy-Ullrich, J. E. (2002). Thrombospondin stimulates focal adhesion disassembly through Gi- and phosphoinositide 3-kinase-dependent ERK activation. *J. Biol. Chem.* **277**, 20453-20460.

Development (2014) 141, 4513-4525 doi:10.1242/dev.109124

Rohlmann, A., Gotthardt, M., Willnow, T. E., Hammer, R. E. and Herz, J. (1996). Sustained somatic gene inactivation by viral transfer of Cre recombinase. *Nat. Biotechnol.* **14**, 1562-1565.

Ryu, Y., Takuwa, N., Sugimoto, N., Sakurada, S., Usui, S., Okamoto, H., Matsui, O. and Takuwa, Y. (2002). Sphingosine-1-phosphate, a platelet-derived lysophospholipid mediator, negatively regulates cellular Rac activity and cell migration in vascular smooth muscle cells. *Circ. Res.* **90**, 325-332.

Soriano, P. (1994). Abnormal kidney development and hematological disorders in PDGF beta-receptor mutant mice. *Genes Dev.* **8**, 1888-1896.

Takayama, Y., May, P., Anderson, R. G. W. and Herz, J. (2005). Low density lipoprotein receptor-related protein 1 (LRP1) controls endocytosis and c-CBL-mediated ubiquitination of the platelet-derived growth factor receptor beta (PDGFR beta). *J. Biol. Chem.* **280**, 18504-18510.

Tallquist, M. D. and Soriano, P. (2000). Epiblast-restricted Cre expression in MORE mice: a tool to distinguish embryonic vs. extra-embryonic gene function. *Genesis* **26**, 113-115.

Tallquist, M. D., French, W. J. and Soriano, P. (2003). Additive effects of PDGF receptor beta signaling pathways in vascular smooth muscle cell development. *PLoS Biol.* **1**, E52.

Zurhove, K., Nakajima, C., Herz, J., Bock, H. H. and May, P. (2008). Gamma-secretase limits the inflammatory response through the processing of LRP1. *Sci. Signal.* **1**, ra15.